

Supplementary Materials

This online supplement contains complementary information on general site characteristics (Table S1), the full rainfall and hydrological data records for the 21 hydrologically active events analysed in this study (Table S2), the general linear model (GLM) configurations applied for studying the surface-patch to hillslope-scale functional connectivity of runoff (Table S3) and sediments (Table S4) in the three experimental slopes, supplementary details on the parameterization of the antecedent precipitation index (API) that was applied in this study (Supplementary Methods S1), and their associated references.

Table of contents:

1. Supplementary Tables.....	page 2
Table S1.....	page 2
Table S2.....	page 3
Table S3.....	page 4
Table S4.....	page 6
2. Supplementary Methods S1.....	page 7
3. References.....	page 10

1. Supplementary Tables

Table S1. General characteristics of the experimental slopes and the soil-surface patch types identified within the slope systems as a function of vegetation composition and soil surface traits. Standard deviation is shown between brackets. Data taken from Merino-Martin et al. (2012; 2015).

	Experimental hillslopes						Soil Surface Patch Types					
	N	Slope 1	Slope 2	Slope 3	N	Ms	Sch	Dg	Tv	Lp	Br	Gs
<i>Slope Topography</i>												
Slope (°)	3	20-40*	20-40*	20*	n/a	n/a	n/a	n/a	n/a	n/a	n/a	n/a
Length (m)	3	70	62	65	n/a	n/a	n/a	n/a	n/a	n/a	n/a	n/a
Aspect	3	North	North	North	n/a	n/a	n/a	n/a	n/a	n/a	n/a	n/a
Berm size (m ²)	3	50	22	n/a	n/a	n/a	n/a	n/a	n/a	n/a	n/a	n/a
<i>Soil Characteristics</i>												
Stoniness (%) †	9	39 (5) A	41 (3) A	42 (3) A	27	41 (11) a	27 (14) ab	17 (4) ab	38 (18) a	7 (9) b	7 (9) b	4 (6) b
Sand (%) †	9	42 (3) A	46 (3) A	44 (3) A	27	32 (2) a	34 (1) a	40 (2) a	44 (1) a	49 (7) a	51 (4) a	52 (1) a
Silt (%) †	9	29 (1) A	25 (1) A	30 (1) A	27	53 (1) a	46 (1) ab	43 (2) ab	38 (2) ab	38 (6) ab	26 (3) b	29 (1) ab
Clay (%) †	9	27 (2) A	30 (2) A	26 (2) A	27	15 (1) a	20 (1) a	17 (1) a	18 (1) a	12 (1) a	20 (1) a	20 (1) a
Organic matter (%) †	9	1.2 (0.3) A	1.6 (0.4) A	2.0 (0.4) A	27	0.3 (0.1) b	0.5 (0.3) ab	1.6 (0.2) ab	2.3 (0.5) ab	2.1 (0.2) ab	2.8 (0.3) ab	4.4 (0.9) a
Total Nitrogen (%) †	9	0.07 (0.02) A	0.10 (0.04) A	0.12 (0.05) A	27	0.03 (0.01) b	0.06 (0.01) ab	0.06 (0.01) ab	0.09 (0.01) ab	0.09 (0.01) ab	0.12 (0.01) ab	0.18 (0.01) a
<i>Vegetation Traits</i>												
Cover (%) ‡‡	105	30 (4) B	45 (4) A	55 (6) A	27	3 (2) b	28 (9) ab	31 (8) ab	34 (5) ab	77 (19) b	93 (9) b	94 (14) b
<i>Hydrological Measurements (Runoff & Soil Erosion)</i>												
Number of plots	3	1	1	1	27	3	6	3	6	3	3	3
Plot size (m ²)	3	498	511	1474	27	1.5	0.8-1.4	0.9-5.1	0.4-3.95	1.7-5.5	1.2-16.4	2.3-3.14
Rill density (m m ⁻²)	3	0.6	0.0	0.0	27	0.0	0.0	0.0	0.0	0.0	0.0	0.0
Runoff coeff. (%) ‡†††	3	14.5	2.1	0.4	27	30.8 (5.4) a	12.8 (9.2) ab	9.8 (2.2) ab	8.4 (2.7) ab	5.9 (2.4) ab	2.0 (2.1) b	0.7 (0.2) b
Erosion (g m ⁻²) ‡†††	3	1824	81	4	27	5212 (1972) a	534 (382) ab	256 (108) ab	234 (91) ab	133 (90) ab	65 (91) b	25 (10) b

Abbreviations: N, number of samples/plots; n/a, not applicable (topographic features were not determined at the patch scale). Names of the dominant plant species for the seven soil surface patch types: Ms, *Medicago sativa*; Sch, *Santolina chamaecyparissus*; Dg, *Dactylis glomerata*; Tv, *Thymus vulgaris*; Lp, *Lolium perenne*; Br, *Brachypodium retusum*; Gs, *Genista scorpius*.

* General slope gradient in the three experimental slopes is 20° except for the berm located at the top 7 and 3 meters of Slopes 1 and 2, respectively, where slope gradient is 40° (see Fig. 1b).

† Measured in three composite samples (each encompassing three randomly distributed subsamples) per slope/surface patch from the top 10 cm of the soil. Soil physico-chemical analyses follow standardized methods by the Spanish Ministry of Agriculture (MAPA, 1994).

‡‡ Green vegetation plus litter. Visually estimated in 0.25 m² plots (35 regularly distributed plots per slope and 6 randomly distributed plots per surface patch).

††† Cumulative values for the study period (October 2007-December 2008).

Different letters indicate significant differences for the three slopes (capital letters) and the seven surface types (lower case letters) at $\alpha=0.05$. Tested using Kruskal-Wallis ANOVA and post-hoc Mann-Whitney U.

Table S2. Hydrological data records applied in this study: rainfall characteristics and (surface patch- and hillslope-scale) hydrological responses for the set of 21 active events recorded during the study period (October 2007–December 2008). Data derived from Merino-Martin et al. (2012).

Date	Dp	Rd†	I ₁₅	I ₃₀	Im††	API†††	Hillslope runoff (mm)			Hillslope sediment yield (g m ⁻²)			Surface patch runoff †††† (mm)						Surface patch sediment yield†††† (g m ⁻²)							
	(mm)	(h)	(mm h ⁻¹)	(mm)	Slp1	Slp2	Slp3	Slp1	Slp2	Slp3	Ms	Sch	Dg	Tv	Lp	Br	Gs	Ms	Sch	Dg	Tv	Lp	Br	Gs		
28/12/07	15.1	14	2	1.5	1.1	0.3	0.0	0.0	0.0	0	0	0.5	<0.1	<0.1	<0.1	0.1	0.1	11	1	1	<1	2	<1	1		
10/01/08	16.1	12	3	1.5	1.3	5.2	0.0	0.0	0.0	0	0	0.3	0.2	<0.1	0.2	0.1	0.1	0.0	5	20	1	6	1	<1	0	
25/01/08	24.7	16	4	3.5	1.6	8.6	0.0	0.0	0.0	0	0	0.8	0.3	<0.1	<0.1	0.1	<0.1	<0.1	<1	<1	<1	<1	<1	<1	<1	
08/03/08	28.9	24	9	5.5	1.2	1.9	<0.1	0.0	0.0	2	0	0.8	0.3	<0.1	<0.1	0.1	0.0	<0.1	2	9	<1	<1	2	0	1	
27/03/08	23.0	17	3	1.5	1.3	5.1	0.0	0.0	0.0	0	0	1.2	0.4	<0.1	0.0	0.1	0.0	0.0	49	5	<1	0	<1	0	0	
13/04/08	24.2	13	9	6.0	1.9	5.5	<0.1	<0.1	0.0	<1	1	0	2.0	0.6	<0.1	<0.1	0.2	0.1	0.1	123	10	<1	<1	1	<1	1
09/05/08	120.1	68	18	15.0	1.8	15.8	17.2	1.0	0.2	187	3	<1	60.8	14.6	7.2	5.9	4.7	1.6	1.1	1553	104	18	27	26	4	4
16/05/08	18.8	7	18	12.0	2.8	106.4	4.4	0.4	<0.1	83	3	<1	4.5	4.0	2.2	1.9	0.0	0.0	0.0	122	23	9	8	0	0	0
18/05/08	73.7	25	16	12.0	3.0	125.1	9.7	3.9	1.2	125	3	1	29.6	14.9	10.1	10.1	4.1	1.3	0.4	547	21	14	12	16	2	8
23/05/08	36.3	16	14	9.5	2.3	144.2	5.4	0.5	0.1	151	20	<1	7.1	3.9	4.3	2.1	2.4	1.2	0.2	443	78	28	20	23	24	1
31/05/08	27.3	15	6	3.5	1.8	63.1	1.4	0.1	0.0	73	1	0	4.5	1.1	0.6	<0.1	0.5	0.0	0.0	115	38	3	<1	2	0	0
09/06/08	48.4	23	11	9.0	2.2	35.6	13.8	2.6	1.3	13	9	1	25.2	13.1	5.5	7.1	3.6	1.4	0.7	323	18	5	16	8	4	2
29/06/08	45.4	18	14	8.5	2.5	41.1	5.0	0.3	<0.1	93	2	<1	12.3	7.6	4.8	4.7	2.1	1.2	0.7	574	32	16	11	8	2	1
17/07/08*	32.5	6	49	32.8	5.7	7.1	4.2	0.8	<0.1	620	27	<1	9.4	12.3	10.2	7.9	2.9	1.3	0.7	216	106	94	56	16	18	3
31/08/08*	16.0	7	11	7.2	2.3	0.3	0.8	0.4	<0.1	215	6	<1	4.3	7.6	4.1	4.6	1.3	1.1	0.3	513	104	46	43	12	3	2
10/06/08	23.0	16	3	2.5	1.4	8.6	2.7	0.2	<0.1	23	2	<1	4.5	3.5	2.5	2.3	0.6	0.5	0.1	115	22	7	13	2	1	<1
12/10/08	13.9	7	11	7.0	2.0	5.1	1.3	0.1	0.0	22	<1	<1	2.6	1.9	1.1	1.7	0.4	0.3	0.1	94	6	4	4	1	1	<1
18/10/08	20.8	9.3	7	5.5	2.2	13.4	2.7	0.2	<0.1	13	<1	<1	4.8	3.6	2.1	1.1	0.7	0.5	0.1	54	14	3	6	1	1	1
24/10/08	17.6	9	11	8.0	2.0	31.5	6.4	0.7	<0.1	64	3	<1	7.1	6.2	4.2	3.6	1.8	0.9	0.1	100	11	3	3	2	3	<1
29/10/08	28.9	17	6	4.5	1.8	49.7	7.5	0.7	<0.1	9	<1	<1	11.2	6.1	3.2	1.7	1.6	0.7	0.2	52	4	1	2	<1	1	<1
02/11/08	43.2	19	12	7.0	2.6	43.3	19.8	2.8	0.2	132	1	<1	23.4	12.0	6.5	5.9	13.7	1.5	0.3	248	12	3	4	11	2	<1

Abbreviations: Dp, storm depth; Rd, rainfall duration; I₁₅, 15-minute maximum rainfall intensity; I₃₀, 30-minute maximum rainfall intensity; Im, mean rainfall intensity; API, antecedent precipitation index (10 days; k= 0.98); Slp, slope. Names of the dominant plant species for the seven soil surface patch types: Ms, *Medicago sativa*; Sch, *Santolina chamaecyparissus*; Dg, *Dactylis glomerata*; Tv, *Thymus vulgaris*; Lp, *Lolium perenne*; Br, *Brachypodium retusum*; Gs, *Genista scorpius*.

† Rainfall duration (Rd) was calculated excluding within-storm gaps >1h showing no rainfall activity.

†† Mean rainfall intensity (Im) was calculated as the ratio of total storm depth (Dp) to rainfall duration (Rd).

††† The antecedent precipitation index (API) was calculated following the formulation by Kohler and Linsley (1951). API antecedent period and scaling factor are T=10 days and k=0.98, respectively (parameters calibrated using local soil moisture records; Appendix B).

†††† Reported data at the patch scale represents the mean runoff and sediment responses recorded in the Gerlach troughs for each event and type of surface patch (Ms, Sch, Dg, Tv, Lp, Br, and Gs).

* Due to raingauge malfunction in the experimental site, Rd, I₁₅ and I₃₀ for these two events were interpolated from two nearby (1 and 4.5 km distance) meteorological stations managed by Viesgo S.L. (Escucha Power station) and the Spanish State Meteorological Agency (9531X code station in Montalbán), respectively.

Table S3. GLM configurations and model statistics (i.e., coefficient of determination, R^2 ; adjusted determination coefficient, Adj R^2 ; and difference in the value of the Akaike Information Criteria between the lowest scoring model and each candidate model, ΔAIC) applied for testing the influence of dynamic rainfall factors (i.e. storm depth, rainfall duration, 15- and 30-min maximum rainfall intensity, mean rainfall intensity, and antecedent precipitation), the structural connectivity of the slope systems and their interactions on the connectivity of runoff for the three experimental slopes. Model configurations are ranked according to ΔAIC . The best supported, most parsimonious model ($\Delta AIC=0$) is highlighted in red.

Model	R^2	Adj R^2	ΔAIC	Model structure†
CR14	0.81	0.78	0.0	$C_R \sim I_{30} + API + \bar{Sc} + \bar{Sc}:I_{30} + \bar{Sc}:API$
CR05	0.78	0.77	0.8	$C_R \sim API + \bar{Sc} + \bar{Sc}:API$
CR33	0.81	0.78	2.5	$C_R \sim I_{15} + I_{30} + API + \bar{Sc} + \bar{Sc}:I_{15} + \bar{Sc}:I_{30} + \bar{Sc}:API$
CR17	0.80	0.77	2.7	$C_R \sim I_{15} + API + \bar{Sc} + \bar{Sc}:I_{15} + \bar{Sc}:API$
CR10	0.79	0.77	4.1	$C_R \sim Dp + API + \bar{Sc} + \bar{Sc}:Dp + \bar{Sc}:API$
CR21	0.79	0.77	4.4	$C_R \sim Im + API + \bar{Sc} + \bar{Sc}:Im + \bar{Sc}:API$
CR36	0.81	0.77	5.3	$C_R \sim I_{30} + Im + API + \bar{Sc} + \bar{Sc}:I_{30} + \bar{Sc}:Im + \bar{Sc}:API$
CR24	0.81	0.77	5.6	$C_R \sim Dp + I_{30} + API + \bar{Sc} + \bar{Sc}:Dp + \bar{Sc}:I_{30} + \bar{Sc}:API$
CR37	0.81	0.77	5.6	$C_R \sim Rd + I_{30} + API + \bar{Sc} + \bar{Sc}:Rd + \bar{Sc}:I_{30} + \bar{Sc}:API$
CR19	0.79	0.76	5.8	$C_R \sim Rd + API + \bar{Sc} + \bar{Sc}:Rd + \bar{Sc}:API$
CR26	0.80	0.76	7.2	$C_R \sim Dp + I_{15} + API + \bar{Sc} + \bar{Sc}:Dp + \bar{Sc}:I_{15} + \bar{Sc}:API$
CR43	0.82	0.77	7.5	$C_R \sim Dp + I_{15} + I_{30} + API + \bar{Sc} + \bar{Sc}:Dp + \bar{Sc}:I_{15} + \bar{Sc}:I_{30} + \bar{Sc}:API$
CR40	0.80	0.76	7.5	$C_R \sim Rd + I_{15} + API + \bar{Sc} + \bar{Sc}:Rd + \bar{Sc}:I_{15} + \bar{Sc}:API$
CR53	0.82	0.77	7.8	$C_R \sim I_{15} + I_{30} + Im + API + \bar{Sc} + \bar{Sc}:I_{15} + \bar{Sc}:I_{30} + \bar{Sc}:Im + \bar{Sc}:API$
CR52	0.82	0.77	7.9	$C_R \sim Rd + I_{15} + I_{30} + API + \bar{Sc} + \bar{Sc}:Rd + \bar{Sc}:I_{15} + \bar{Sc}:I_{30} + \bar{Sc}:API$
CR39	0.80	0.76	8.1	$C_R \sim I_{15} + Im + API + \bar{Sc} + \bar{Sc}:I_{15} + \bar{Sc}:Im + \bar{Sc}:API$
CR41	0.80	0.76	8.2	$C_R \sim Rd + Im + API + \bar{Sc} + \bar{Sc}:Rd + \bar{Sc}:Im + \bar{Sc}:API$
CR31	0.80	0.76	8.4	$C_R \sim Dp + Im + API + \bar{Sc} + \bar{Sc}:Dp + \bar{Sc}:Im + \bar{Sc}:API$
CR27	0.80	0.76	8.7	$C_R \sim Dp + Rd + API + \bar{Sc} + \bar{Sc}:Dp + \bar{Sc}:Rd + \bar{Sc}:API$
CR47	0.81	0.76	9.3	$C_R \sim Dp + Rd + I_{30} + API + \bar{Sc} + \bar{Sc}:Dp + \bar{Sc}:Rd + \bar{Sc}:I_{30} + \bar{Sc}:API$
CR46	0.81	0.76	9.8	$C_R \sim Dp + I_{30} + Im + API + \bar{Sc} + \bar{Sc}:Dp + \bar{Sc}:I_{30} + \bar{Sc}:Im + \bar{Sc}:API$
CR55	0.81	0.76	9.8	$C_R \sim Rd + I_{30} + Im + API + \bar{Sc} + \bar{Sc}:Rd + \bar{Sc}:I_{30} + \bar{Sc}:Im + \bar{Sc}:API$
CR57	0.82	0.76	11.9	$C_R \sim Dp + Rd + I_{15} + I_{30} + API + \bar{Sc} + \bar{Sc}:Dp + \bar{Sc}:Rd + \bar{Sc}:I_{15} + \bar{Sc}:I_{30} + \bar{Sc}:API$
CR59	0.82	0.76	12.2	$C_R \sim Dp + I_{15} + I_{30} + Im + API + \bar{Sc} + \bar{Sc}:Dp + \bar{Sc}:I_{15} + \bar{Sc}:I_{30} + \bar{Sc}:Im + \bar{Sc}:API$
CR48	0.80	0.75	12.2	$C_R \sim Dp + Rd + I_{15} + API + \bar{Sc} + \bar{Sc}:Dp + \bar{Sc}:Rd + \bar{Sc}:I_{15} + \bar{Sc}:API$
CR62	0.82	0.76	12.2	$C_R \sim Rd + I_{15} + I_{30} + Im + API + \bar{Sc} + \bar{Sc}:Rd + \bar{Sc}:I_{15} + \bar{Sc}:Im + \bar{Sc}:API$

Abbreviations: C_R , per-rainfall-event functional connectivity of runoff; Dp, storm depth; Rd, rainfall duration; I_{15} , 15-minute maximum rainfall intensity; I_{30} , 30-minute maximum rainfall intensity; Im, mean rainfall intensity; API, antecedent precipitation index (10 days; $k = 0.98$); \bar{Sc} , mean structural connectivity of “source areas” of the slopes.

†, tested models take log-transformed values for the co-variables Dp, Rd, I_{15} , I_{30} , Im and API.

Table S3 continuation (1).

Model	R ²	Adj R ²	ΔAIC	Model structure†
CR51	0.80	0.75	12.3	$C_R \sim Dp + Rd + Im + API + \bar{Sc} + \bar{Sc}:Dp + \bar{Sc}:Rd + \bar{Sc}:Im + \bar{Sc}:API$
CR56	0.80	0.75	12.3	$C_R \sim Rd + I_{15} + Im + API + \bar{Sc} + \bar{Sc}:Rd + \bar{Sc}:I_{15} + \bar{Sc}:Im + \bar{Sc}:API$
CR49	0.80	0.75	12.4	$C_R \sim Dp + I_{15} + Im + API + \bar{Sc} + \bar{Sc}:Dp + \bar{Sc}:I_{15} + \bar{Sc}:Im + \bar{Sc}:API$
CR60	0.82	0.75	14.1	$C_R \sim Dp + Rd + I_{30} + Im + API + \bar{Sc} + \bar{Sc}:Dp + \bar{Sc}:Rd + \bar{Sc}:I_{30} + \bar{Sc}:Im + \bar{Sc}:API$
CR61	0.81	0.74	16.3	$C_R \sim Dp + Rd + I_{15} + Im + API + \bar{Sc} + \bar{Sc}:Dp + \bar{Sc}:Rd + \bar{Sc}:I_{15} + \bar{Sc}:Im + \bar{Sc}:API$
CR63	0.82	0.75	17.2	$C_R \sim Dp + Rd + I_{15} + I_{30} + Im + API + SC + \bar{Sc}:Dp + \bar{Sc}:Rd + \bar{Sc}:I_{15} + \bar{Sc}:I_{30} + \bar{Sc}:Im + \bar{Sc}:API$
CR09	0.61	0.56	43.8	$C_R \sim Dp + Rd + \bar{Sc} + \bar{Sc}:Dp + \bar{Sc}:Rd$
CR30	0.64	0.57	44.5	$C_R \sim Dp + Rd + Im + \bar{Sc} + \bar{Sc}:Dp + \bar{Sc}:Rd + \bar{Sc}:Im$
CR11	0.60	0.55	45.3	$C_R \sim Dp + Im + \bar{Sc} + \bar{Sc}:Dp + \bar{Sc}:Im$
CR07	0.60	0.55	45.9	$C_R \sim Dp + I_{30} + \bar{Sc} + \bar{Sc}:Dp + \bar{Sc}:I_{30}$
CR02	0.56	0.53	46.0	$C_R \sim I_{30} + \bar{Sc} + \bar{Sc}:I_{30}$
CR01	0.56	0.52	46.3	$C_R \sim Dp + \bar{Sc} + \bar{Sc}:Dp$
CR20	0.60	0.54	46.5	$C_R \sim Rd + Im + \bar{Sc} + \bar{Sc}:Rd + \bar{Sc}:Im$
CR08	0.59	0.54	46.8	$C_R \sim Dp + I_{15} + \bar{Sc} + \bar{Sc}:Dp + \bar{Sc}:I_{15}$
CR03	0.54	0.51	48.2	$C_R \sim I_{15} + \bar{Sc} + \bar{Sc}:I_{15}$
CR13	0.58	0.53	48.6	$C_R \sim Rd + I_{30} + \bar{Sc} + \bar{Sc}:Rd + \bar{Sc}:I_{30}$
CR45	0.65	0.56	49.2	$C_R \sim Dp + Rd + I_{30} + Im + \bar{Sc} + \bar{Sc}:Dp + \bar{Sc}:Rd + \bar{Sc}:I_{30} + \bar{Sc}:Im$
CR25	0.61	0.54	49.6	$C_R \sim Dp + Rd + I_{15} + \bar{Sc} + \bar{Sc}:Dp + \bar{Sc}:Rd + \bar{Sc}:I_{15}$
CR23	0.61	0.54	49.6	$C_R \sim Dp + Rd + I_{30} + \bar{Sc} + \bar{Sc}:Dp + \bar{Sc}:Rd + \bar{Sc}:I_{30}$
CR50	0.65	0.55	50.1	$C_R \sim Dp + Rd + I_{15} + Im + \bar{Sc} + \bar{Sc}:Dp + \bar{Sc}:Rd + \bar{Sc}:I_{15} + \bar{Sc}:Im$
CR06	0.53	0.50	50.1	$C_R \sim Im + \bar{Sc} + \bar{Sc}:Im$
CR16	0.57	0.52	50.1	$C_R \sim Rd + I_{15} + \bar{Sc} + \bar{Sc}:Rd + \bar{Sc}:I_{15}$
CR12	0.57	0.51	50.6	$C_R \sim I_{15} + I_{30} + \bar{Sc} + \bar{Sc}:I_{15} + \bar{Sc}:I_{30}$
CR28	0.61	0.53	50.8	$C_R \sim Dp + I_{30} + Im + \bar{Sc} + \bar{Sc}:Dp + \bar{Sc}:I_{30} + \bar{Sc}:Im$
CR29	0.61	0.53	51.0	$C_R \sim Dp + I_{15} + Im + \bar{Sc} + \bar{Sc}:Dp + \bar{Sc}:I_{15} + \bar{Sc}:Im$
CR22	0.60	0.52	51.4	$C_R \sim Dp + I_{15} + I_{30} + \bar{Sc} + \bar{Sc}:Dp + \bar{Sc}:I_{15} + \bar{Sc}:I_{30}$
CR35	0.60	0.52	51.9	$C_R \sim Rd + I_{30} + Im + \bar{Sc} + \bar{Sc}:Rd + \bar{Sc}:I_{30} + \bar{Sc}:Im$
CR15	0.56	0.50	51.9	$C_R \sim I_{30} + Im + \bar{Sc} + \bar{Sc}:I_{30} + \bar{Sc}:Im$
CR38	0.60	0.52	52.1	$C_R \sim Rd + I_{15} + Im + \bar{Sc} + \bar{Sc}:Rd + \bar{Sc}:I_{15} + \bar{Sc}:Im$
CR58	0.66	0.54	52.8	$C_R \sim Dp + Rd + I_{15} + I_{30} + Im + \bar{Sc} + \bar{Sc}:Dp + \bar{Sc}:Rd + \bar{Sc}:I_{15} + \bar{Sc}:I_{30} + \bar{Sc}:Im$
CR18	0.55	0.49	53.8	$C_R \sim I_{15} + Im + \bar{Sc} + \bar{Sc}:I_{15} + \bar{Sc}:Im$
CR32	0.59	0.50	54.0	$C_R \sim Rd + I_{15} + I_{30} + \bar{Sc} + \bar{Sc}:Rd + \bar{Sc}:I_{15} + \bar{Sc}:I_{30}$
CR42	0.62	0.52	54.3	$C_R \sim Dp + Rd + I_{15} + I_{30} + \bar{Sc} + \bar{Sc}:Dp + \bar{Sc}:Rd + \bar{Sc}:I_{15} + \bar{Sc}:I_{30}$

Abbreviations: C_R , per-rainfall-event functional connectivity of runoff; Dp , storm depth; Rd , rainfall duration; I_{15} , 15-minute maximum rainfall intensity; I_{30} , 30-minute maximum rainfall intensity; Im , mean rainfall intensity; API , antecedent precipitation index (10 days; $k = 0.98$); \bar{Sc} , mean structural connectivity of “source areas” of the slopes.

†, tested models take log-transformed values for the co-variables Dp , Rd , I_{15} , I_{30} , Im and API .

Table S3 continuation (2).

Model	R ²	Adj R ²	ΔAIC	Model structure†
CR44	0.61	0.51	55.9	$C_R \sim Dp + I_{15} + I_{30} + Im + \bar{Sc} + \bar{Sc}:Dp + \bar{Sc}:I_{15} + \bar{Sc}:I_{30} + \bar{Sc}:Im$
CR34	0.57	0.48	56.4	$C_R \sim I_{15} + I_{30} + Im + \bar{Sc} + \bar{Sc}:I_{15} + \bar{Sc}:I_{30} + \bar{Sc}:Im$
CR54	0.61	0.50	57.0	$C_R \sim Rd + I_{15} + I_{30} + Im + \bar{Sc} + \bar{Sc}:Rd + \bar{Sc}:I_{15} + \bar{Sc}:I_{30} + \bar{Sc}:Im$
CR04	0.45	0.41	59.7	$C_R \sim Rd + \bar{Sc} + \bar{Sc}:Rd$

Abbreviations: C_R , per-rainfall-event functional connectivity of runoff; Dp , storm depth; Rd , rainfall duration; I_{15} , 15-minute maximum rainfall intensity; I_{30} , 30-minute maximum rainfall intensity; Im , mean rainfall intensity; API, antecedent precipitation index (10 days; $k=0.98$); \bar{Sc} , mean structural connectivity of “source areas” of the slopes.

†, tested models take log-transformed values for the co-variables Dp , Rd , I_{15} , I_{30} , Im and API.

Table S4. GLM configurations and model statistics (i.e., coefficient of determination, R²; adjusted determination coefficient, Adj R²; and difference in the value of the Akaike Information Criteria between the lowest scoring model and each candidate model, ΔAIC) applied for testing the influence of dynamic rainfall factors (i.e. storm depth, rainfall duration, 15- and 30-min maximum rainfall intensity, mean rainfall intensity, and antecedent precipitation), the structural connectivity of the slope systems and their interactions on the connectivity of runoff for the three experimental slopes. Model configurations are ranked according to ΔAIC. The best supported, most parsimonious model (ΔAIC=0) is highlighted in red.

Model	R ²	Adj R ²	ΔAIC	Model structure
CS04	0.81	0.79	0.0	$C_S \sim Im + \bar{Sc} + \bar{Sc}:Im$
CS08	0.81	0.78	4.4	$C_S \sim I_{15} + Im + \bar{Sc} + \bar{Sc}:I_{15} + \bar{Sc}:Im$
CS10	0.81	0.78	4.6	$C_S \sim Im + API + \bar{Sc} + \bar{Sc}:Im + \bar{Sc}:API$
CS06	0.81	0.78	5.4	$C_S \sim I_{30} + Im + \bar{Sc} + \bar{Sc}:I_{30} + \bar{Sc}:Im$
CS02	0.79	0.77	6.4	$C_S \sim I_{15} + \bar{Sc} + \bar{Sc}:I_{15}$
CS09	0.80	0.77	7.9	$C_S \sim I_{15} + API + \bar{Sc} + \bar{Sc}:I_{15} + \bar{Sc}:API$
CS05	0.80	0.77	8.2	$C_S \sim I_{15} + I_{30} + \bar{Sc} + \bar{Sc}:I_{15} + \bar{Sc}:I_{30}$
CS14	0.82	0.78	8.2	$C_S \sim I_{15} + Im + API + \bar{Sc} + \bar{Sc}:I_{15} + \bar{Sc}:Im + \bar{Sc}:API$
CS12	0.82	0.78	8.5	$C_S \sim I_{15} + I_{30} + Im + \bar{Sc} + \bar{Sc}:I_{15} + \bar{Sc}:I_{30} + \bar{Sc}:Im$
CS11	0.82	0.77	8.7	$C_S \sim I_{15} + I_{30} + API + \bar{Sc} + \bar{Sc}:I_{15} + \bar{Sc}:I_{30} + \bar{Sc}:API$
CS13	0.81	0.77	9.7	$C_S \sim I_{30} + Im + API + \bar{Sc} + \bar{Sc}:I_{30} + \bar{Sc}:Im + \bar{Sc}:API$
CS15	0.83	0.77	11.4	$C_S \sim I_{15} + I_{30} + Im + API + \bar{Sc} + \bar{Sc}:I_{15} + \bar{Sc}:I_{30} + \bar{Sc}:Im + \bar{Sc}:API$
CS01	0.76	0.74	14.0	$C_S \sim I_{30} + \bar{Sc} + \bar{Sc}:I_{30}$
CS07	0.78	0.74	16.2	$C_S \sim I_{30} + API + \bar{Sc} + \bar{Sc}:I_{30} + \bar{Sc}:API$
CS03	0.43	0.37	69.3	$C_S \sim API + \bar{Sc} + \bar{Sc}:API$

Abbreviations: C_R , per-rainfall-event functional connectivity of runoff; Dp , storm depth; Rd , rainfall duration; I_{15} , 15-minute maximum rainfall intensity; I_{30} , 30-minute maximum rainfall intensity; Im , mean rainfall intensity; API, antecedent precipitation index (10 days; $k=0.98$); \bar{Sc} , mean structural connectivity of “source areas” of the slopes.

2. Supplementary Methods S1

These supplementary methods contain information on the parameterization of the Antecedent Precipitation Index applied in this study as a proxy of the antecedent wetness conditions for the experimental slopes and study period

2.1. Objective

The Antecedent Precipitation Index (API; Kohler and Linsley, 1951) provides a practical proxy of antecedent wetness conditions in hydrological studies where no continuous records of soil moisture at daily/sub-daily frequency are available for analysis. Overall, API represents antecedent wetness as a weighted summation of daily (antecedent) precipitation:

$$API = \sum_{t=-1}^{-T} P_t k^{-t} \quad (S1)$$

where, P_t (mm) is the precipitation on a given day t , k is a dimensionless decay coefficient that represents a measure of the decline in the influence of past precipitation on soil moisture, and T (days) is the antecedent period considered for the calculation of the index. For general convention, k typically takes a value between 0.85 and 0.98 (Viessman and Lewis, 1996). The number of antecedent days, T , considered for the calculation of the index is generally between 5 and 15 days (Viessman and Lewis, 1996; NRCS, 1997; Hong et al., 2007; Ali et al., 2010; Masselink et al., 2016).

The objective of this complementary analysis was to parameterize the k coefficient and T antecedent period of the index for the three experimental slopes and the full duration of the study (from October 2007 to December 2008) covered in our analysis.

2.2. Data and Methods

We applied time-domain-reflectometry (TDR) volumetric records of soil moisture (%, vol/vol) obtained from autumn 2007 to winter 2008 in the three experimental slopes to

parameterize the API k and T parameters for this study. The records were taken periodically (every 15 days without rain and within 5 days after each runoff-producing rainfall event) in a set of 32 soil-moisture profiles (12 profiles per experimental slope) equipped with TDR sensors that were installed at 5-, 25- and 50-cm depth (Merino-Martín et al., 2015).

The recorded soil moisture values and precipitation records for the study period in the three experimental slopes (Figure S1) evidenced the formation of two markedly dry intervals in autumn/winter 2007-08 and summer 2008, and two wet phases running in spring and autumn 2008.

We evaluated the Pearson' R correlation between the soil moisture series of the slopes and a variety of API series obtained by using different values for the k (0.80-0.98 range) and T (from 5 to 15 days) parameters. The k and T values that maximized the correlation between soil moisture and API were selected as calibration values for the API parameters.

2.3. API parameterization results

The highest correlation score between the observed values of soil moisture and the calculated API values was reached for all the three slopes for $k= 0.98$ and $T= 10$ days (Figure S2 a-c). Using these numbers as calibrated values for the API parameters, API explains a high proportion of the variance comprised by the soil moisture data in the experimental slopes (the R^2 for the obtained optimal soil moisture-API relationships ranges 0.76-0.80 for the three experimental slopes; Figure S2 d-f).

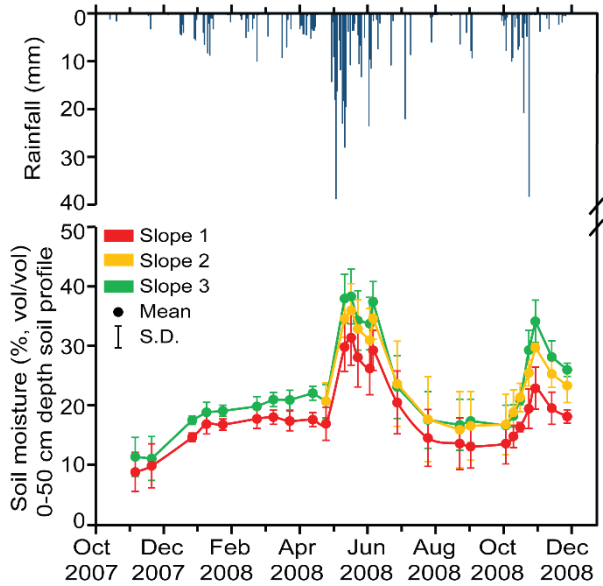


Figure S1. Precipitation and soil moisture records during the study period

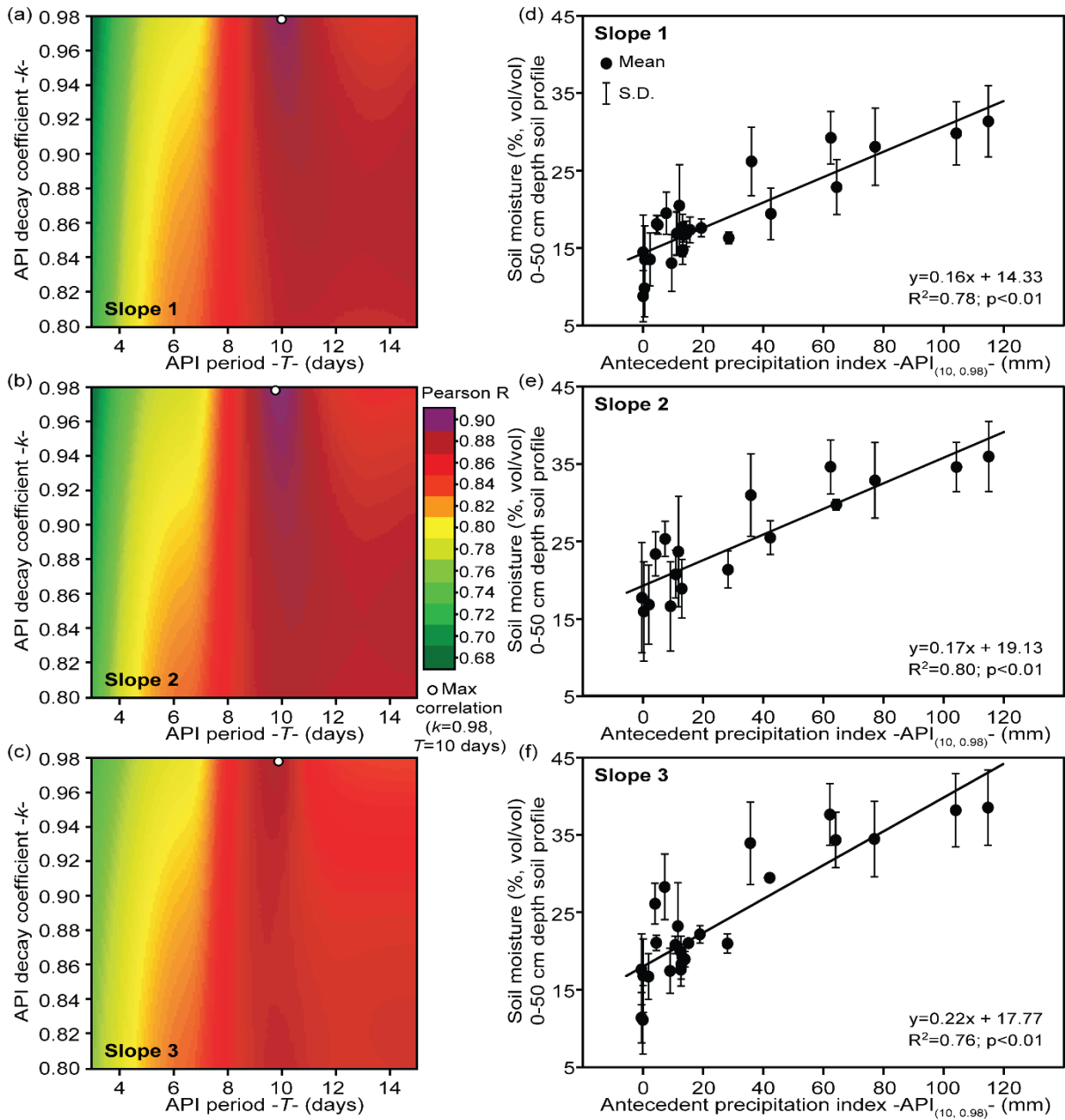


Figure S2. Determination of optimal k and T values: (a-c) Pearson's R correlation coefficients for the relationships between soil moisture and API in the three experimental slopes using different k and T values for the computation of API values, and (d-f) moisture-API relationship for the determined optimal k and T values (0.98 and 10 days, respectively) in the three experimental slopes.

3. References

- Ali, S., Ghosh, N. C., and Singh, R.: Rainfall-runoff simulation using a normalized antecedent precipitation index, *Hydrological Sciences Journal*, 55, 266-274, <https://doi.org/10.1080/02626660903546175>, 2010.
- Hong, Y., Adler, R. F., Hossain, F., Curtis, S., and Huffman, G. J.: A first approach to global runoff simulation using satellite rainfall estimation, *Water Resources Research* 43, W08502, <https://doi.org/10.1029/2006WR005739>, 2007.
- Kohler, M. A., and Linsley, R. K.: Predicting the runoff from storm rainfall, *Weather Bureau Research Papers* 34, US Department of Commerce, Washington, 1951.
- MAPA: *Métodos Oficiales de Análisis*, Secretaría General de Alimentación, Dirección de Política Alimentaria, Ministerio de Agricultura, Pesca y Alimentación, Madrid, 1994.
- Masselink, R. J. H., Keesstra, S. D., Temme, A. J. A. M., Seeger, M., Giménez, R., and Casalí, J.: Modelling discharge and sediment yield at catchment scale using connectivity components, *Land Degradation and Development*, 27, 933-945, <https://doi.org/10.1002/ldr.2512>, 2016.
- Merino-Martín, L., Moreno-de las Heras, M., Pérez-Domingo, S., Espigares, T., and Nicolau, J. M.: Hydrological heterogeneity in Mediterranean reclaimed slopes: runoff and sediment yield at the patch and slope scales along a gradient of overland flow, *Hydrology and Earth System Sciences* 16, 1305-1320, <https://doi.org/10.5194/hess-16-1305-2012>, 2012.
- Merino-Martín, L., Moreno-de las Heras, M., Espigares, T., and Nicolau, J. M.: Overland flow directs soil moisture and ecosystem processes at patch scale in Mediterranean restored slopes, *Catena* 133, 71-84, <https://doi.org/10.1016/j.catena.2015.05.002>, 2015.
- NRCS: *National Engineering Handbook, Part 630: Hydrology*, US Department of agriculture, Natural Resources Conservation Service, Washington, 1997.
- Viessman, W., and Lewis, G. L.: *Introduction to Hydrology*, Harper Collins, New York, 1996.